The bridging conformations of double-end anchored polymer-surfactants destabilize a hydrogel of lipid membranes

N. L. Slack
Materials and Physics Departments, Biochemistry and Molecular Biology Program, University of California, Santa Barbara, California 93106

P. Davidson
Materials and Physics Departments, Biochemistry and Molecular Biology Program, University of California, Santa Barbara, California 93106 and Laboratoire de Physique des Solides (CNRS), Bat. 510, Universite Paris Sud, 91405 Orsay, France

M. A. Chibbaro
Materials and Physics Departments, Biochemistry and Molecular Biology Program, University of California, Santa Barbara, California 93106

C. Jeppesen
Materials Research Laboratory, University of California, Santa Barbara, California 93106

P. Eiselt and H. E. Warriner
Materials and Physics Departments, Biochemistry and Molecular Biology Program, University of California, Santa Barbara, California 93106

H.-W. Schmidt
Materials and Physics Departments, Biochemistry and Molecular Biology Program, University of California, Santa Barbara, California 93106 and Makromolekulare Chemie I and Bayreuther Institut für Makromolekulforschung (BIMF), Universität Bayreuth, 95440 Bayreuth, Germany

P. Pincus and C. R. Safinya
Materials and Physics Departments, Biochemistry and Molecular Biology Program, University of California, Santa Barbara, California 93106

(Received 26 April 2001; accepted 12 July 2001)

Double-end-anchored poly-ethylene-glycol-surfactants (DEA-PEG-surfactants) induce the gelation of lyotropic lamellar L_α phases stabilized by undulation forces. The physical hydrogel ($L_{\alpha,g}$) derives its viscoelasticity from the proliferation of defects at a mesoscopic level. The DEA-PEG-surfactants assume both looping and bridging conformations. The existence of novel bridging conformations is indicated by the coexistence of two lamellar phases and the limited swelling of the L_α and $L_{\alpha,g}$ phases. Modeling of the polymer decorated membranes demonstrates the existence of bridging and yields a rapidly decreasing density of bridging conformations with increasing interlayer spacing. © *2001 American Institute of Physics.* [DOI: 10.1063/1.1399061]

I. INTRODUCTION

Hydrogels of polymer networks constitute a very important class of ''soft'' matter materials with applications which span diverse areas from the food industry to the medical and biotechnological industries in implants, tissue replacements, and drug delivery systems.[1,2] Here, we describe a new type of lamellar hydrogel based on fluid lipid membranes (rather than polymers) with added low molecular weight poly(ethylene glycol) anchored to the membrane at each end with a hydrophobic chain (double-end-anchored-PEG). X-ray diffraction shows unambiguously that these lipid based two-dimensional membranes are in the fluid state which further distinguishes them from solid two-dimensional polymers of block copolymer systems.

Hydrophobically modified polymers obtained by chemically grafting one or several hydrophobic moieties onto a hydrophilic polymer have proven of particular interest to the biomedical drug delivery field since it was shown that they could protect drug and gene containing ''stealth'' liposomes (consisting of closed concentric lipid membrane shells coated with polymer) from the human immune system.[3,4] The polymer is believed to make the liposome biocompatable by effectively repelling immune cells due to a polymer brush type steric repulsion.[5–8] Moreover, flexible and fluid surfactant bilayers incorporating such macromolecules mimic, to some extent, biological membranes that are covered with polysaccharide polymer coils used for cell signaling.[9]

Doping the swollen L_α phase of the dimyristoylphosphatidylcholine (DMPC), pentanol, and water system with small amounts of poly(ethylene glycol) (PEG) chains substituted at one end by a hydrophobic moiety was recently shown to induce a new class of physical gels.[10–13] This work with single-end-anchored PEG-surfactants (SEA-PEG-surfactants) prompted us to synthesize a double-end-anchored (DEA) PEG-surfactant by chemically grafting a hydrophobic moiety at each end of the PEG chain.[14] Such polymers strongly differ from the SEA-PEG-surfactants in

that they may assume both looping and bridging conformations [Fig. 1(b)]. The looping conformations are so far thought to be the most probable ones and give rise to a repulsive interaction between membranes, whereas the bridging ones give rise to an attractive interaction.[15,16] If present, the bridging conformations are therefore expected to deeply modify the microstructure of the lamellar phase. In this letter, we first show that these double-end-anchored PEG-surfactants (DEA-PEG-surfactants) also induce the gelation of the swollen L_α phase. Then, we describe experimental and theoretical evidence of the existence of bridging conformations derived from the detailed inspection of phase diagrams. Finally, we report results from a theoretical model which demonstrate conclusively that the bridging conformation alters the phase behavior of these systems.

The paper is organized as follows: Sec. II gives a description of the materials, the x-ray diffraction setup, and the rheological apparatus used in this study. Section III describes the results of the phase diagram and a qualitative model of bridging and looping conformations of double-end-anchored polymers. Section IV concludes with a brief discussion of the importance of this study.

II. EXPERIMENT

A. Sample preparation

The chemical synthesis and characterization of the DEA-PEG-surfactants have already been described in detail.[14] The chemical structure for the DEA-PEG-surfactants investigated here are shown in Fig. 1(a).

Dimyristoylphosphatidylcholine (DMPC), 677.94 g/mol, $\rho_{\mathrm{DMPC}}=1.1$ g/cm^3, of a purity >99% was purchased from Avanti Polar Lipids Inc. (Alabaster, AL), and pentanol, 88.15 g/mol, $\rho_{\mathrm{pentanol}}=0.81$ g/cm^3 of purity 99% was purchased from Sigma Chemical Corp. Both of these components were used without further purification. Purified 18 MΩ water was obtained in house through a Milli-Q Plus unit (Millipore Corp., Bedford, MA).

The definitions and equations given below were used to determine the composition of each sample. For all equations, g_x is the weight in grams of material x. In Eq. (3), the factor of 2 multiplying the PEG concentrations accounts for the double-end-anchor nature of the molecule. For every DEA PEG-surfactant molecule, two surfactant groups will be present in the membrane,

$$g_{\mathrm{total}}=g_{\mathrm{water}}+g_{\mathrm{PEG\text{-}surfactant}}+g_{\mathrm{DMPC}}+g_{\mathrm{pentanol}}, \tag{1}$$

$$\Phi_w=\frac{g_{\mathrm{water}}}{g_{\mathrm{total}}}(\text{weight fraction of water}), \tag{2}$$

$$c_{\mathrm{PEG\text{-}surfactant}}=100*\left[\frac{2*(g_{\mathrm{PEG\text{-}surfactant}}/MW_{\mathrm{PEG\text{-}surfactant}})}{2*(g_{\mathrm{PEG\text{-}surfactant}}/MW_{\mathrm{PEG\text{-}surfactant}})+g_{\mathrm{DMPC}}/MW_{\mathrm{DMPC}}}\right], \tag{3}$$

$$\frac{g_{\mathrm{pentanol}}}{MW_{\mathrm{pentanol}}}=4*\left(2*\frac{g_{\mathrm{PEG\text{-}surfactant}}}{MW_{\mathrm{PEG\text{-}surfactant}}}+\frac{g_{\mathrm{DMPC}}}{MW_{\mathrm{DMPC}}}\right). \tag{4}$$

All samples were prepared by directly mixing the components in test tubes, as described previously.[10–13] A constant molar ratio of pentanol to surfactant molecules (DMPC +PEG-surfactant) of 4.0±0.5 [Eq. (4)] was maintained to ensure that the surfactant chains would always be in the melted state.[17] This then also isolates the effect of PEG-surfactant on the fluidity, bending rigidity, and shape of the membrane. The remaining compositional degrees of freedom are the volume fraction of water (Φ_w) and the ratio of the PEG-surfactant to total surfactant (c_{PEG}). We noticed that these mixtures are stable over time scales ranging from a few months up to a year depending on composition.

B. Phase determination

The phase behavior of each sample was determined by a simple inversion test. Any sample that did not flow for at least 5 s under its own weight after inversion of the test tube was considered a gel. Previous studies of the SEA-PEG-surfactants have shown that this operational definition provides a consistent criterion which agrees quite well with the more quantitative rheological measurements.[13] Samples were also examined on a macroscopic scale in polarized light to check for the nematiclike texture which is a signature of the gel phase.[10,11,13]

C. X-ray diffraction

X-ray scattering studies were performed on a Huber four-circle diffractometer using an 18 kW Rigaku rotating anode generator (Rigaku, Danvers, MA) (Cu K_α, λ=1.54 Å), a cylindrically bent focusing pyrolitic graphite (002) monochromator and a Bicron point detector (Bicron, Newbury, OH, USA). The in-plane resolution, defined using slits, was $\delta q=0.01-0.015$ Å^{-1}, and the out-of-plane resolution was $\delta q=0.14-0.3$ Å^{-1}; scan stepsize was generally 0.001 Å^{-1}. Additional experiments were carried out at the Stanford

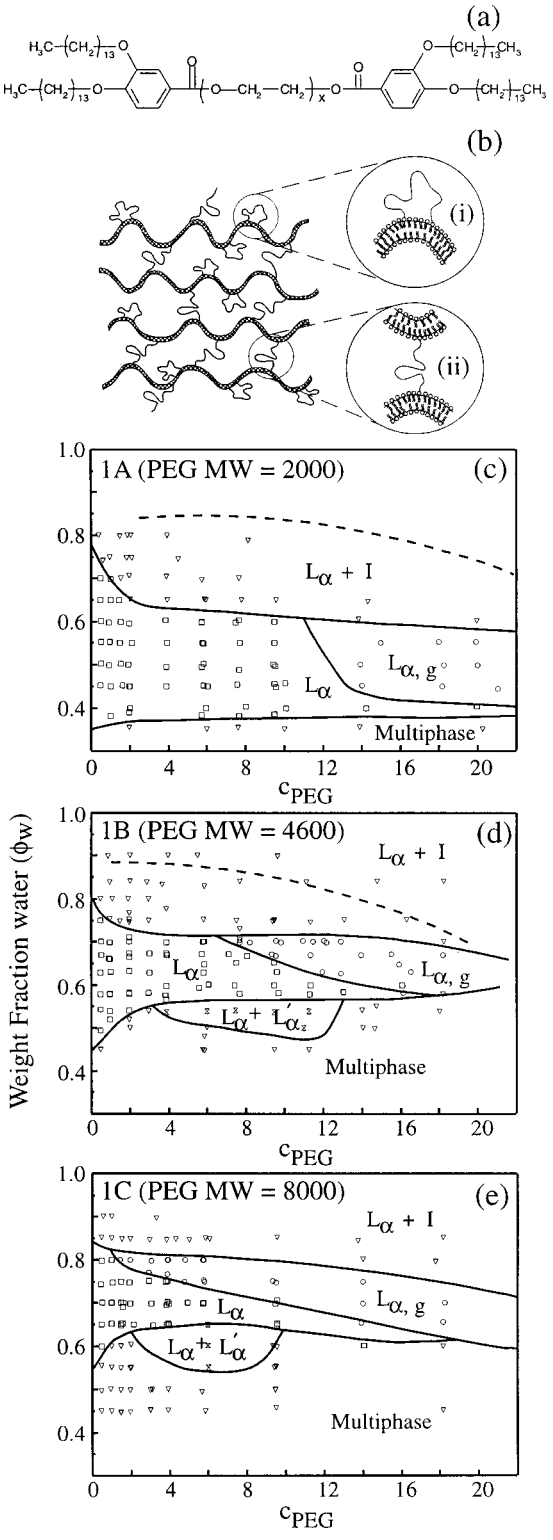

FIG. 1. (a) Chemical structure of the DEA-PEG-surfactants. $x=45$ for **1A**, $x=104$ for **1B**, $x=181$ for **1C**. (b) Schematic of undulating membranes composed of a lipid (DMPC), a cosurfactant (pentanol), and DEA-PEG-surfactants demonstrating the two different configurations of the DEA-PEG-surfactant: looping (i) and bridging (ii). The phase diagrams of the DMPC, pentanol, water, and DEA-PEG-surfactant systems for the PEG-surfactant **1A** (c), **1B** (d), and **1C** (e). The water weight fraction, ϕ_w, is plotted vs the concentration of PEG-surfactant c_{PEG} [2* mol PEG surfactant/(2*mol PEG surfactant + mol DMPC)*100]. Phase boundaries are distinguished by solid lines. The dashed lines in (c) and (d) denote the upper two phase boundary of the single-end-anchored PEG-surfactant of equivalent length (Ref. 11).

Synchrotron Radiation Laboratory on beamline 10-2 using either a Bicron point detector or a 180 mm MAR image-plate 2D x-ray detector (Mar Industries, San Diego, CA, USA). A Si (111) double bounce monochromator was used at 8 keV with focus at the sample position. In the Bicron experiments, in-plane resolution, again defined by slits, was $\delta q = 0.0014-0.0028$ Å^{-1}, and the out-of-plane resolution was $\delta q = 0.01-0.02$ Å^{-1}; scan stepsize was usually 0.0005 Å^{-1}. For the 2D detector experiments, resolution was defined by the detector pixel size and the distance from sample to detector. Images were radially averaged to produce powder scans with a stepsize of 0.0007 Å^{-1} and a radially averaged resolution of 0.0027 Å^{-1}. Exposure times were typically 1–2 h.

For all experiments, samples were sealed in either quartz or glass 1.5 mm x-ray capillary tubes (Charles Supper Co., Natick, MA, USA). These capillary tubes were then set on a translation stage for automatic data acquisition.

D. Rheology

Constant-stress oscillatory shear-strain experiments were carried out with a Rheometrics dynamic stress rheometer, model 1710C (Rheometrics, Piscataway, NJ, USA), in the cone and plate geometry with a 40 mm diam plate, a cone angle of 0.04 rad, and a gap size of 0.05 mm. For this geometry, a minimum volume of 0.7 cm^3 is recommended. In our experiments, a volume of 1–1.5 cm^3 was used. In order to minimize evaporation during testing, a small housing was placed around the set up which enclosed pentanol and water-soaked cotton balls. All experiments were performed at room temperature.

Samples were subjected to three different tests. In order to establish the regime of linear viscoelasticity, we performed a dynamic stress sweep test in which the stress is increased from about 0.6 to 100 dyn/cm^2 at a frequency of 1 Hz. Within this regime, each sample was tested in a transient single point test to ensure the sinusoidal strain response followed the sinusoidal stress by a phase angle. Finally, a dynamic frequency sweep test was run at a constant stress over a frequency range of 0.01 to 10 Hz to determine both the real (storage elasticity) modulus, G', and the imaginary (loss) modulus, G''. For each sample, two sets of tests were run. The first set included the dynamic stress sweep test, the transient single point test, and the dynamic frequency sweep test. In the second set of tests, the sample was replaced with fresh sample from the same test tube and only the dynamic frequency sweep test was run. This second dynamic frequency sweep test was used to check the reproducibility of the first set of tests. In particular, we wished to ensure that the dynamic moduli were not merely products of alignment produced during the high stresses imposed by the dynamic stress sweep test.

III. RESULTS

The phase diagrams obtained with the three DEA-PEG-surfactants are qualitatively similar (Fig. 1). They all show a large region of a stable lamellar phase bounded by multiphase regions located, respectively, at low and high water

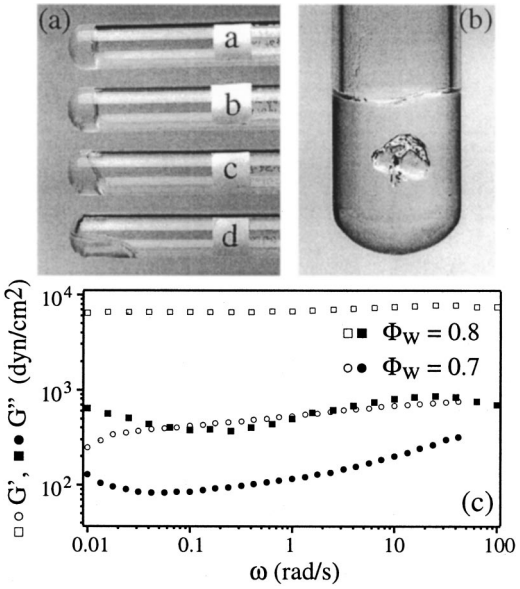

FIG. 2. (a) A series of test tubes containing mixtures of DMPC, pentanol, water, and PEG-surfactant **1C** tilted horizontally to illustrate the gelation transition: (a) a gel $L_{\alpha,g}$ phase containing $c_{\mathrm{PEG}}=14\%$ and $\phi_w=0.75$; (b) a gel $L_{\alpha,g}$ phase containing $c_{\mathrm{PEG}}=14\%$ and $\phi_w=0.70$; (c) a fluid L_α phase containing $c_{\mathrm{PEG}}=14\%$ and $\phi_w=0.65$; (d) a fluid L_α phase containing $c_{\mathrm{PEG}}=14\%$ and $\phi_w=0.60$. (b) A gel $L_{\alpha,g}$ phase sample containing $c_{\mathrm{PEG}}=4.85\%$ (**1C**) and $\phi_w=0.75$ supporting a nonspherical bubble displays strong elasticity. (c) Rheological data of a fluid L_α sample containing $c_{\mathrm{PEG}}=4.85\%$ (**1C**) and $\phi_w=0.70$ (circles) and a gel $L_{\alpha,g}$ sample containing $c_{\mathrm{PEG}}=4.85\%$ (**1C**) and $\phi_w=0.80$ (squares). G' is denoted by open symbols and G'' is denoted by closed symbols. The elastic modulus increases by over one order of magnitude upon gelation, and for the gel sample, remains one order of magnitude greater than the loss modulus over the frequency range examined.

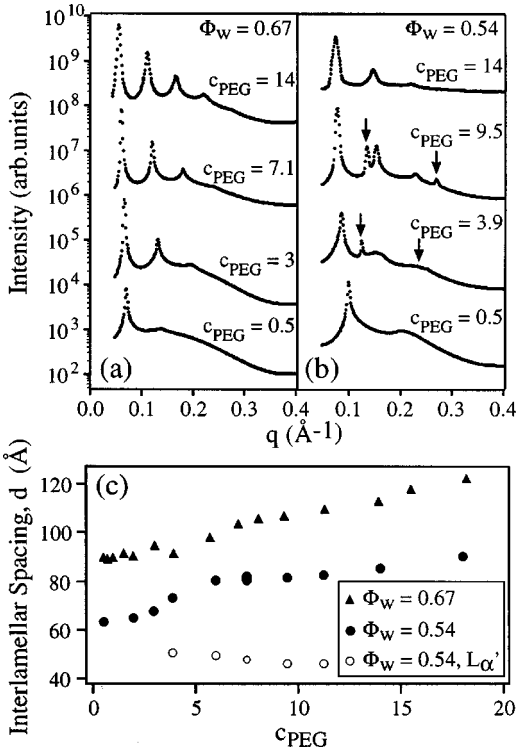

FIG. 3. X-ray scattering powder scans of mixtures of DMPC, pentanol, water, and PEG-surfactant **1B**. (a) Samples of constant $\phi_w=0.67$ and $c_{\mathrm{PEG}}=0.5\%$ (fluid L_α); $c_{\mathrm{PEG}}=3\%$ (fluid L_α); $c_{\mathrm{PEG}}=7.1\%$ (fluid L_α); $c_{\mathrm{PEG}}=14\%$ (gel $L_{\alpha,g}$) show that there is no structural phase transition at the onset of gelation. (b) Samples of constant $\phi_w=0.54$ and $c_{\mathrm{PEG}}=0.5\%$ (fluid L_α); $c_{\mathrm{PEG}}=3.9\%$ [fluid $L_\alpha+L'_\alpha$ (arrows)]; $c_{\mathrm{PEG}}=9.5\%$ [fluid $L_\alpha+L'_\alpha$ (arrows)]; $c_{\mathrm{PEG}}=14\%$ (fluid L_α+isotropic phase) reveal the existence of a region of coexistence between two lamellar phases of different interlamellar spacing. (c) A plot of interlamellar spacing vs c_{PEG} **1B** for increasing PEG-surfactant at constant $\phi_w=0.67$ (triangles) and $\phi_w=0.54$ (circles). The closed circles denote the L_α phase found at higher ϕ_w and the open circles denote the second L_α phase referred to as L'_α.

concentrations. The lamellar region is itself divided by a gel transition above which the lamellar phase shows elasticity (Fig. 2) and is then called $L_{\alpha,g}$. The properties of the $L_{\alpha,g}$ phase are very different from those of conventional hydrogels based on polymer networks but are similar to those of the $L_{\alpha,g}$ phase obtained from the SEA-PEG-surfactants.[10–13] More precisely, it is obtained by diluting the fluid L_α phase with water, and less DEA-PEG-surfactant is needed to achieve gelation as Φ_w increases. Further, the swollen lamellar L_α phase of these hydrogels are stabilized by Helfrich entropic repulsion[17–19] instead of electrostatic interactions.[20] The $L_{\alpha,g}$ phase has a finite yield stress and its elastic modulus G' ($\approx 10^4$ dyn/cm^2) is larger than the viscous modulus G'' by about an order of magnitude over the whole frequency range probed by rheology [Fig. 2(c)]. X-ray diffraction (XRD) data on powder samples show that the $L_{\alpha,g}$ phase retains the lamellar L_α symmetry [Fig. 3(a)]. Moreover, scans of samples of increasing PEG-surfactant concentrations reveal an increasing number of lamellar harmonics, indicating an extra polymer-induced intermembrane repulsion. However, no major change occurs at the gelation transition, which indicates that gelation does not arise from this extra repulsion. In fact, optical microscopy in polarized light of gel samples reveals the proliferation of tiny line defects, which may even show nematic ordering on a macroscopic length scale.[14] All these experimental observations prove that the gelation of the fluid L_α phase by doping with DEA-PEG-surfactants is due to the same mechanism as that which prevails upon doping with SEA-PEG-surfactants.[10–13]

However, close examination of the phase diagrams obtained with the three DEA-PEG-surfactants reveals two important features that are not observed with SEA-PEG-surfactants. First, the phase diagrams of compounds **1B** and **1C** [Figs. 1(d) and 1(e)] differ from those obtained with SEA-PEG-surfactants of equivalent molecular weight by the fact that they have a region, at low water content, where two lamellar L_α phases coexist. This is best illustrated by the XRD scans [Fig. 3(b)] of a series of samples of increasing c_{PEG} at constant Φ_w. This series of scans shows the existence of two sets of lamellar reflections of different periods in a given range of c_{PEG}. The coexistence of the two lamellar phases can also be detected by optical microscopy. Indeed, even though these samples just show a common L_α texture in polarized light, they show a large contrast in natural light due to the difference in refractive indices of the two phases (data not shown). The phase diagrams obtained with SEA-PEG-surfactants only showed coexistence of a lamellar phase with an isotropic one which could simply be explained by the fact that a minimum swelling is required for the polymer chain to insert into the intermembrane aqueous medium.

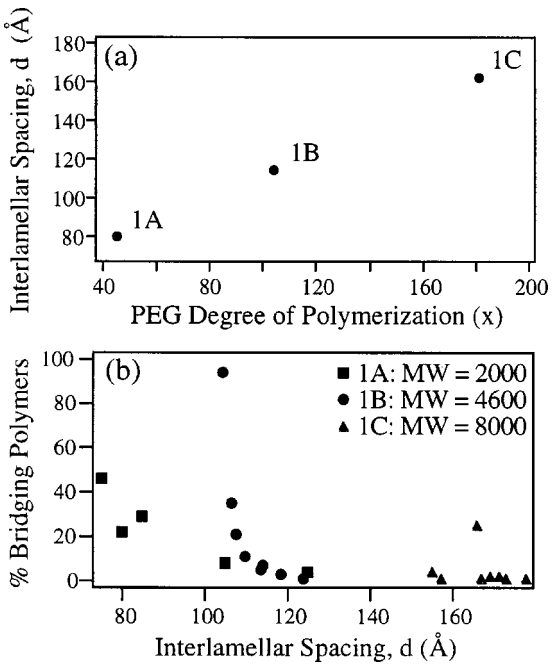

FIG. 4. (a) A plot of the maximum interlamellar spacing at $c_{\mathrm{PEG}}=6\%$ as a function of PEG degree of polymerization demonstrating the strong dependence of maximum swelling on the PEG molecular weight. (b) A plot of the percentage of bridging polymers vs interlamellar spacing obtained from computer simulations. The rapidly decreasing density of bridging conformations with increasing interlamellar spacing is obvious.

This situation is actually observed when doping the L_α phase with compound **1A**. In the case of compounds **1B** and **1C**, the two L_α phases are easily distinguished by their very different spacing variations as c_{PEG} is increased. The L_α phase which is also found at higher Φ_w has a period increasing with c_{PEG}, whereas the other one, called L'_α, has a period slightly decreasing with c_{PEG} [Fig. 3(c)]. It should be noted though that the period of the additional L'_α phase is clearly larger than the bilayer thickness ($\delta\approx 29$ Å) so that this phase cannot be described as a collapsed stack of membranes. The L'_α phase probably arises from the appearance of a polymer mediated attractive interaction involving bridging and partially adsorbed conformations. A possible explanation for the coexistence of these two L_α phases is that the L_α phase of larger period would be richer in looping conformations, whereas the other one would be richer in bridging conformations [Fig. 1(b)]. The former L_α phase would experience an extra repulsive interaction due to the loops thus leading to the larger period. In contrast, the bridging conformations of the L'_α phase would give rise to an attractive interaction, thus reducing the lamellar period. In this latter phase, the PEG coils may even be partially adsorbed onto the membranes.

Further, the maximum swelling of the L_α phase is very reduced compared to that achieved with SEA-PEG-surfactants as demonstrated by the shift of the upper two-phase boundary to lower Φ_w [dashed lines, Figs. 1(c) and 1(d)]. The nature of this boundary can be understood by examining the XRD scans of samples of increasing water fractions at constant c_{PEG}. These scans show that the lamellar period, *d*, increases regularly throughout the lamellar region according to the usual one-dimensional swelling behavior. This swelling behavior allows us to estimate the bare membrane thickness, $\delta\sim 29$ Å, which agrees well with previous determinations.[18] Once the upper two-phase boundary is reached, *d* remains constant demonstrating the expulsion of excess water from the lamellar phase. Further, the shift of the upper two-phase boundary strongly depends on PEG molecular weight as the swelling of the L_α phase doped with the DEA-PEG-surfactant of lowest PEG mass is the most reduced. The dependence of the maximum lamellar period on PEG molecular weight is shown in Fig. 4(a). In stark contrast, the location of this boundary does not depend on PEG molecular weight in the case of the SEA-PEG-surfactants [dashed lines, Figs. 1(c) and 1(d)]. The decreased stability of the lamellar phase upon doping with small amounts of DEA-PEG-surfactants is evidence for the existence of an appreciable proportion of bridging conformations of the PEG coils. At the microscopic level, these bridging conformations will effectively crosslink neighboring membranes and therefore will resist swelling by the solvent, thus setting a limit on the maximum value of Φ_w. It is also clear that the effect on the phase diagram of these bridging conformations seems to be strongest for the lowest PEG molecular weight. Indeed, longer PEG coils can accommodate larger swelling with comparatively less stretching. In fact, the average membrane separation at maximum swelling, $d_{w\ \max}$, can be calculated from the measured maximum lamellar period and from the bilayer thickness, and should then be compared with the PEG coil gyration radius, R_g. For instance, at $c_{\mathrm{PEG}}\approx 6\%$, $d_{w\ \max}$ is ~51 Å for **1A**, ~85 Å for **1B** and ~133 Å for **1C**. The values of R_g can be estimated using the simple scaling law, $R_g\approx a x^{3/5}$, where $a=3.6$ Å is the monomer length;[21] R_g is ~35 Å for **1A**, ~58 Å for **1B**, and ~81 Å for **1C**. The ratio of $d_{w\ \max}$ to R_g increases from about 1.45 for **1A** and **1B** to about 1.6 for **1C**. The elastic energy stored in the stretched PEG coils is $F_{\mathrm{el}}\propto kT(d_{w\ \max}/R_g)^2$ to a first approximation.[21] This means that, at maximum swelling, each PEG coil has stored a few *kT*. Recent theoretical studies have suggested that the configurational entropy of the looping conformations should be larger than the entropy of the bridging ones. So it could be assumed that most PEG coils would adopt the looping conformations. Nevertheless, our observations provide clear evidence that the free energy of the bridging conformations is certainly not much larger than that of the looping ones. Note that the ideas developed in this section may also be relevant to the field of block copolymers, in particular when discussing swollen ABA triblock copolymers.[22–24]

Further evidence of the existence of the cross-bridging conformation is garnered from a theoretical model. Assuming a single polymer picture with well ordered lamella, a gross mean-field theory approach for the energy per unit area of membrane as a function of *d* spacing can be written as

$$E(d)=\rho^* E_\gamma(d-\delta)+E_{\mathrm{H}}(d)+E_{\mathrm{vdw}}(d), \tag{5}$$

where $E_{\mathrm{H}}(d)$ is the Helrich undulation energy, $E_{\mathrm{vdw}}(d)$ is the van der Waals energy, $E_\gamma(d-\delta)$ is the energy of stretching the PEG molecule to length $d-\delta=d_w$, and ρ is the density of bridging polymers. The expression for the Helfrich and van der Waals energies can be obtained from previous work

on membrane interactions.[25,26] A numerical result for the first energy term [Eq. (5)] is obtained through a computer simulation modeled after Jeppesen *et al.*[27] The remaining variable ρ is determined by first plotting E using the experimentally determined d spacing and a chosen ρ. The ρ for each sample is then determined by altering ρ to shift the minimum of the energy curve until it corresponds to the experimentally determined d spacing. The values for ρ obtained by this method are then compared to the overall concentration of PEG/unit area of membrane in each sample. For the **1A** and **1B** systems, it was found that the percentage of bridging polymers was inversely proportional to d spacing suggesting that it is the presence of cross-bridging polymers which limits the swelling of the L_α phase for these systems [Fig. 4(b)]. The percentage of bridging polymers was found to be relatively insensitive to d spacing for the **1C** system. However, the model may not be valid for this system because the restoring force E_γ is negligible. In samples containing **1C**, the polymer part of the DEA-PEG-surfactant molecule is 181 repeat units long suggesting that polymer–polymer and polymer–membrane interactions can no longer be ignored and must be accounted for in a more sophisticated theory.

IV. DISCUSSION AND CONCLUSIONS

Our experimental results are consistent with and demonstrate the importance of looping and bridging conformations of double-end-anchored PEG-surfactants on the resulting microstructure of the lamellar L_α phase. The DEA-PEG-surfactants induce a new case of coexistence of two fluid lamellar phases that we believe are rich respectively in looping and bridging conformations. Moreover, although these polymer–surfactants can still induce gelation of the L_α phase, its range of stability upon dilution is clearly reduced, due to the bridging conformations which crosslink neighboring membranes.

The system we report on is of importance in the field of biophysics and biotechnology. Virtually all systemic applications (i.e., direct delivery of biomolecules into the blood stream) of vesicles for drug and gene delivery applications utilize PEG-surfactant based molecules. This is because PEG-surfactants coat the delivery vehicle (e.g., a vesicle or a multilamellar vesicle) in a manner which leads to the repulsion of immune cells attacking the vesicle. However, the precise structure at the water–membrane interface is still unclear and a subject of much discussion. Thus, any new fundamental knowledge about the behavior of these types of chainlike macromolecules near membrane interfaces, including the new double-end-anchored PEG-surfactants reported in this paper, which clearly alters intermembrane interactions, is extremely important.

The mean field model is intended as a first qualitative estimate to show how the concentration of bridging polymer conformations can be calculated from (static) energetic considerations, when the lipid membranes are arranged in a lamellae. This model should be a reasonable guide under the conditions of low polymer concentrations, negligible contributions to the energetic balance from (polymer) looping conformations, and polymer–polymer interaction.

ACKNOWLEDGMENTS

The authors acknowledge helpful and pleasant discussions with R. Lipowsky and J. F. Joanny. This work is supported by NIH GM59288, NSF-DMR-9972246, and the UC-Biotechnology Research and Education Program (99-14). The Materials Research Laboratory at U.C. Santa Barbara is supported by NSF Grant No. DMR-9632716 and DMR-0080034.

[1] See, e.g., D. DeRossi, K. Kajiwara, Y. Osada, and A. Yamauchi, *Polymer Gels: Fundamentals and Biomedical Applications* (Plenum, New York, 1991).
[2] N. A. Peppas and R. Langer, Science **263**, 1715 (1994).
[3] D. D. Lasic and F. J. Martin, *Stealth Liposomes* (CRC, Boca Raton, 1995).
[4] D. D. Lasic, *Liposomes in Gene Delivery* (CRC, Boca Raton, 1997).
[5] S. Alexander, J. Phys. (France) **38**, 977 (1977).
[6] P.-G. deGennes, J. Phys. (France) **37**, 1443 (1976).
[7] P.-G. deGennes, Macromolecules **13**, 1069 (1980).
[8] S. T. Milner, Science **251**, 905 (1991).
[9] H. Lodish, D. Baltimore, A. Berk, S. L. Zipursky, P. Matsudaira, and J. Darnell, *Molecular Cell Biology*, 3rd ed. (Freeman, New York, 1995).
[10] H. E. Warriner, S. H. J. Idziak, N. L. Slack, P. Davidson, and C. R. Safinya, Science **271**, 969 (1996).
[11] H. E. Warriner, P. Davidson, N. L. Slack, M. Schellhorn, P. Eiselt, S. H. J. Idziak, H. W. Schmidt, and C. R. Safinya, J. Chem. Phys. **107**, 3707 (1997).
[12] S. L. Keller, H. E. Warriner, C. R. Safinya, and J. A. Zasadzinski, Phys. Rev. Lett. **78**, 4781 (1997).
[13] H. E. Warriner, S. L. Keller, S. H. J. Idziak, N. L. Slack, P. Davidson, J. A. Zasadzinski, and C. R. Safinya, Biophys. J. **75**, 272 (1998).
[14] N. L. Slack, M. Schellhorn, P. Eiselt, M. A. Chibbaro, U. Schulze, H. E. Warriner, P. Davidson, H. W. Schmidt, and C. R. Safinya, Macromolecules **31**, 8503 (1998).
[15] R. Lipowsky, Phys. Rev. Lett. **77**, 1652 (1996).
[16] R. Lipowsky, Colloids Surf., A **128**, 255 (1997).
[17] C. R. Safinya, D. Roux, G. S. Smith, S. K. Sinha, P. Dimon, N. A. Clark, and A. M. Bellocq, Phys. Rev. Lett. **57**, 2718 (1986).
[18] C. R. Safinya, E. B. Sirota, D. Roux, and G. S. Smith, Phys. Rev. Lett. **62**, 1134 (1989).
[19] F. Castro-Roman, G. Porte, and C. Ligoure, Phys. Rev. Lett. **82**, 109 (1999).
[20] D. Roux and C. R. Safinya, J. Phys. (France) **49**, 307 (1988).
[21] P.-G. de Gennes, *Scaling Concepts in Polymer Physics* (Cornell University Press, Ithaca, 1991).
[22] E. B. Zhulina and A. Halperin, Macromolecules **25**, 5730 (1992).
[23] M. W. Matsen, J. Chem. Phys. **102**, 3884 (1995).
[24] B. Li and E. Ruckenstein, Macromol. Theory Simul. **7**, 333 (1998).
[25] W. Helfrich, Z. Naturforsch. A **33**, 305 (1978).
[26] *Micelles, Membranes, Microemulsions, and Monolayers*, edited by W. M. Gelbart, A. Ben-Shaul, and D. Roux (Springer-Verlag, New York, 1994).
[27] C. Jeppesen, J. Y. Wong, T. L. Kuhl, J. N. Israelachvili, N. Mullah, S. Zalipsky, and C. M. Marques, Science **293**, 465 (2001).